

# Spectroscopic characterization of molecular interdiffusion at a poly(vinyl pyrrolidone)/vinyl ester interface

Christelle M. Laot, Eva Marand\*, Hideko T. Oyama

NSF Science and Technology Center for High Performance Polymeric Adhesives and Composites, Department of Chemical Engineering, Virginia Polytechnic Institute and State University, Blacksburg, VA 24061, USA

Received 2 October 1997; accepted 23 February 1998

## Abstract

The molecular interdiffusion across a poly(vinyl pyrrolidone)/vinyl ester monomer (PVP/VE) interface was investigated in situ by Fourier transform infrared attenuated total reflectance (FTi.r.-ATR) spectroscopy. In order to separate the effects of the vinyl ester monomer diffusion and the VE crosslinking reaction, ATR experiments were carried out at temperatures below the normal curing temperature of the VE. The infrared bands at 1717 and 1507  $\text{cm}^{-1}$ , characteristic of the vinyl ester monomer, and the bands at 1669 and 1419  $\text{cm}^{-1}$ , characteristic of the PVP, were used in a quantitative analysis. Diffusion coefficients were determined by following intensity variations in these selected characteristic bands as a function of time, and fitting this data to a Fickian model. A mutual diffusion coefficient on the order of  $2 \times 10^{-8} \text{ cm}^2/\text{s}$  was calculated at 100°C. Although the magnitude of the diffusion coefficients obtained was consistent with values found in the literature for diffusion of small molecules in polymers, the simple one-dimensional Fickian diffusion model employed as a first approximation had some limitations for the particular (PVP/VE) system. Because the glass transition temperature of PVP changed as diffusion proceeded, the mutual diffusion coefficient should not stay constant. In fact, it was shown that the  $T_g$  can drop by as much as 140°C during the diffusion process. © 1998 Elsevier Science Ltd. All rights reserved.

**Keywords:** FTi.r.-ATR spectroscopy; Diffusion; Interface

## 1. Introduction

Polymer composites play an increasingly important role in today's technology. Composites based on carbon fibre and vinyl ester matrix are being employed mainly in aerospace and structural applications. Vinyl ester monomers used in thermoset polymer matrix composites [1–3] are typically diluted with styrene, since the vinyl ester does not flow well at room temperature. Styrene is a good diluent since it is miscible with the vinyl ester and is relatively inexpensive. The vinyl ester monomer forms a three-dimensional network with the styrene, when cross-linked via free radical copolymerization by opening of the double bonds C=C on the ends of the monomer, leading to an addition reaction with no formation of by-products. Vinyl ester monomers diluted with styrene can be fully cured at low temperature very rapidly [4].

However, carbon fibre reinforced composites, simply composed of carbon fibre and vinyl ester matrix, show poor mechanical properties, which arise as a result of poor

adhesion between the fibre and the matrix [5]. Mechanical properties of woven-carbon fibre/thermoset–resin composites can be greatly improved if the interphase between the reinforcing high-strength low-weight fibre and the matrix is made more compliant. In order to improve the adhesion of the vinyl ester matrix to the carbon fibre, a thermoplastic coating such as poly(vinyl pyrrolidone) (PVP) can be used as an intermediate sizing material between the matrix and the fibre, although epoxy pre-polymers are more common. Carbon fibres are usually coated with the sizing material and therefore the sizing material has to be compatible with the carbon fibre surface and miscible with the vinyl ester matrix. After contact is established between the PVP and the vinyl ester matrix, adhesion takes place by interdiffusion across the interface [6]. The incorporation of PVP coated carbon fibres in highly crosslinked thermosets improves the toughness, without compromising modulus, strength and chemical resistance [7]. The extent of mutual diffusion at the (sizing material/polymer matrix) interphase plays a critical role in determining the mechanical properties of the composite.

\* Corresponding author.

The diffusion at the PVP/vinyl ester resin interface has been studied by Oyama et al. [8] using electron microprobe analysis (EMP). In this technique, electron bombardment generates characteristic X-rays, which can yield qualitative and quantitative information about the composition of the interface [9]. The bilayer films made up of PVP and vinyl ester resin were cured at a temperature of 150°C. The normalized PVP concentration profile was obtained as a function of curing time by EMP using nitrogen in PVP as a probe. The image of the interface region was also obtained by this method. Two regions with different diffusion coefficients were observed in the interphase, and this can be attributed to partial plasticization of PVP by the resin [8]. Different vinyl ester–styrene compositions were also studied and it was found that the interfacial thickness increased dramatically with the amount of styrene content. Although very valuable, the EMP analysis method presents some limitations. Since EMP determines the composition using elements as probes in order to determine the interfacial structure, the system has to contain a characteristic element to distinguish between two phases. Furthermore, the EMP method requires that the samples be in a solid state. As a consequence, the diffusion of the vinyl ester monomer at the initial cure stage before the gel point cannot be measured, and special care has to be taken [10] since the electron beam sometimes damages the polymer surface. The lateral resolution of this technique is about 1  $\mu\text{m}$  [10]. Other methods, which can be used to obtain the mutual diffusion coefficient between polymers, include Rutherford back-scattering spectrometry [11], forward recoil spectrometry [12], neutron reflection spectroscopy [13], scanning infrared microscopy [14], scanning electron microscopy with energy-dispersive X-ray spectrometry [15], and dynamic light scattering [16]. Each of these methods has its own limitations and permits the measurement of the diffusion coefficients over a particular range, at a given penetration depth. These techniques usually allow one to determine the concentration profile as a function of depth. However, in some cases it is not possible to study certain polymeric materials when the atomic compositions are not distinguishable. Labeling is, therefore, required and this may modify the value of the diffusion coefficient. Furthermore, some of the methods are destructive.

A non-destructive technique, Fourier transform infrared attenuated total reflectance (FTi.r.-ATR) spectroscopy has been successfully applied in the last decade to measure diffusion coefficients in polymers in real time. Van Alsten and Lustig [17] derived the equations for measuring mutual diffusion coefficients of polymers in melts, such as polystyrene and poly(methyl methacrylate), provided that the diffusion behaviour was totally Fickian. Jabbari and Peppas [18–20] concentrated their analysis on the interdiffusion of polystyrene (PS) and poly(vinyl methyl ether) (PVME), i.e. polymers with very dissimilar mobilities. It was found that after contact was established between the two polymers, the faster diffusing component swelled the

slower diffusing component, prior to mutual interdiffusion across the interface. This swelling, considered as a non-Fickian case II process, and confirmed by dynamic mechanical analysis (DMTA), gave rise to unsymmetric concentration profiles in the interface. The results were analyzed with a combination of Fickian and case II models at temperatures just below and above the glass transition temperature of the slower diffusing component. Case II diffusion occurs when the diffusion is very rapid compared with the polymer relaxation time and is characterized by a moving interface. The diffusion is independent of the concentration profile, since it depends on the relaxation time of the slower component. Consequently, the diffusion coefficient is time dependent. Jabbari and Peppas have further demonstrated that for the PS/PVME system at 15°C below the  $T_g$  of the PS, the percentage of non-Fickian behaviour was close to 70%, whereas at 5°C above the  $T_g$  of the PS, this percentage was close to 20%. This suggests that diffusion coefficients can change drastically near a  $T_g$ . Comparison of the PS/PVME system with a system consisting of polystyrene and poly(isobutyl vinyl ether), PiBVE [21], was also carried out. While the PS/PVME system involved compatible polymers, the PS/PiBVE system consisted of incompatible polymers.

In the case of diffusion behaviour of small molecules in polymers, FTi.r.-ATR results of diffusion studies were found to be consistent with those of other techniques [22–26]. Fieldson and Barbari [22] measured the diffusion of water in polyacrylonitrile below and above the glass transition temperature of the polymer and found a good agreement with the values reported in the literature employing other techniques. Good agreement between gravimetric sorption, nuclear magnetic resonance and ATR measurements [23] was found for the acetone–polypropylene, methanol–polystyrene and methanol–poly(methyl methacrylate) systems. Farinas et al. [24] analyzed the diffusion of urea into a silicone polymer and showed that the results were consistent with bulk transport techniques. Semwal et al. [25] also reported a good agreement between the ATR method and a weight gain method for the diffusion of sulfur mustard and oxygen mustard in polypropylene and biaxial-oriented polypropylene. Hong et al. [26] measured the diffusion of methyl ethyl ketone in polyisobutylene by vapor sorption FTi.r.-ATR spectroscopy and emphasized that the method led to consistent results, compared with a conventional gravimetric sorption balance. The ATR technique offers several advantages, such as the ability to monitor the diffusion in situ, provided that the compounds have some infrared distinguishable absorption bands. It is also possible to work in a broad range of temperatures and with a wide variety of interface combinations. The ATR method can be used to measure diffusion coefficients over a wide range of values, from  $1 \times 10^{-5}$  to  $1 \times 10^{-16}$   $\text{cm}^2/\text{s}$ , as well as to simultaneously monitor physical interactions and chemical reactions occurring within the polymeric system.

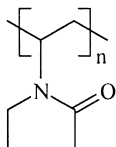


Fig. 1. Repeat unit of poly(vinyl pyrrolidone).

The purpose of the present work is to investigate the molecular interdiffusion across a poly(vinyl pyrrolidone)/vinyl ester monomer (PVP/VE) interface using ATR spectroscopy. Analysis of selected characteristic bands permitted the tracking of diffusion of both components. In order to separate the effects of the vinyl ester monomer diffusion and the cross-linking reaction, ATR experiments were carried out at temperatures below the normal curing temperature. The effect of styrene on the value of the diffusion coefficient has not been investigated at this time, even though the commercial vinyl ester resin contains styrene as a diluent.

## 2. Experimental

The infrared spectra were obtained on a BIO-RAD FTS-40A spectrometer. The spectrometer was equipped with a liquid nitrogen cooled mercury–cadmium–telluride (MCT) detector. Spectra were collected at a resolution of  $4\text{ cm}^{-1}$  with 64 averaged scans. The temperature of the sample was measured with a thermocouple and regulated at  $\pm 0.1^\circ\text{C}$  with an OMEGA<sup>®</sup> Model CN-2011TC-DC1 programmable controller. Spectral manipulations were performed using a software, developed by Galactic Industries Corporation called GRAMS/386<sup>™</sup>.

A Seagull<sup>™</sup>-ATR attachment bought from Harrick Scientific Corporation was used. This attachment requires a hemispherical single internal reflection element (IRE), having a 25 mm diameter and a height of 12.5 mm. The IRE crystal was made from zinc selenide, having a refractive index of 2.42. The critical angle of the system,  $\theta_c$ , was  $39.21^\circ$  and hence to avoid spectral distortions, the angle of incidence was chosen as  $45^\circ$ .

Poly(vinyl pyrrolidone) PVP K90, corresponding to a viscosity-average molecular weight of 1 100 000 g/mol, or a degree of polymerization of 9910, was supplied by BASF Corporation. The repeat unit is shown in Fig. 1. The refractive index of PVP is 1.53, as listed in the Polymer Handbook [27].

The vinyl ester monomer (VE) was obtained from Dow Chemical Co. Its structure is shown in Fig. 2. The vinyl ester oligomer had a number average molecular weight equal to 690 g/mol ( $x$  is equal to 1.65), and was not diluted with styrene. However, it contained an inhibitor, 1, 4-benzoquinone. The inhibitor was added in order to prevent eventual gelation at ambient temperature. VE had to be heated to a temperature of about  $50^\circ\text{C}$  in order to take an aliquot. The monomer did not show signs of polymerization below  $125^\circ\text{C}$ , as determined by DSC experiments.

The thin film of PVP was cast directly from solution onto the ATR crystal, in order to develop a good contact between the polymer and the ATR crystal. Since PVP was soluble in water, a small amount of the dried PVP was dissolved in water at a concentration of 6% by weight. The system was stirred for 2 h to ensure complete mixing. A film of the liquid PVP was deposited directly onto the ATR crystal by spin coating. The film was first dried at room temperature and then dried under vacuum, in order to allow the water to evaporate. The thickness of the PVP film, measured via profilometry, was typically on the order of  $3\ \mu\text{m}$ . A thick film of VE of about 0.5 mm was placed on an aluminium foil. The thin PVP film was pressed against the thick VE layer. The sample was then clamped in a heating cell and placed in the ATR attachment. The heating cell, purchased from Harrick Scientific, could be operated up to  $200^\circ\text{C}$ .

Differential scanning calorimetry (DSC) measurements were conducted using a Perkin-Elmer differential calorimeter. Solutions of PVP and VE in methanol were mixed together to achieve different compositions and dried under vacuum to evaporate all the solvent. It was verified that no characteristic bands of methanol appeared in the infrared spectra of the blends. Each sample was held for 3 min at  $-80^\circ\text{C}$ , heated from  $-80^\circ$  to  $70^\circ\text{C}$  at a heating rate of  $10^\circ\text{C}/\text{min}$ , held for 3 min at  $70^\circ\text{C}$ , cooled from  $70^\circ$  to  $-80^\circ\text{C}$  at  $100^\circ\text{C}/\text{min}$ , held for 3 min at  $-80^\circ\text{C}$ , and heated again from  $-80^\circ$  to  $70^\circ\text{C}$  at  $10^\circ\text{C}/\text{min}$ . The glass transition temperatures of the blends were determined from the second heating.

## 3. Results

### 3.1. Spectroscopic data

In order to follow the diffusion of specific components, distinguishable infrared bands had to be identified for the

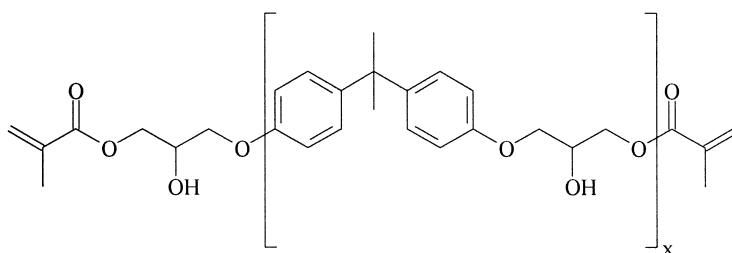


Fig. 2. Structure of the vinyl ester monomer.

two components. Fig. 3 shows the FTi.r.-ATR overlapped spectra of pure PVP and VE in the mid-infrared region at room temperature. The analysis was restricted to typical group vibrations in the spectral region from 1750 to 1350  $\text{cm}^{-1}$ . The bands at 1717 and 1507  $\text{cm}^{-1}$ , characteristic of the vinyl ester monomer, and the bands at 1669 and 1419  $\text{cm}^{-1}$ , characteristic of the poly(vinyl pyrrolidone), were used in quantitative analysis of the spectra. The bands with peak locations at 1717 and 1669  $\text{cm}^{-1}$  were attributed to the carbonyl stretch of VE and PVP, respectively. The absorption frequency at 1669  $\text{cm}^{-1}$  is quite low for a carbonyl band, but this is due to the fact that this band contains not only contributions from C=O stretching vibrations, but also from N–C vibrations [28]. The band at 1507  $\text{cm}^{-1}$  has been assigned to the aromatic ring stretches of the VE, whereas the band at 1419  $\text{cm}^{-1}$  is attributed to the CH deformation of the cyclic  $\text{CH}_2$  groups in the PVP [29]. The ATR experiments were carried out as a function of time at three different temperatures, namely 80°, 90° and 100°C, in order to assess the temperature dependence of the diffusion coefficient. Fig. 4 shows the evolution of the spectra with time at 100°C. As interdiffusion proceeds, the absorbances of VE bands at 1717 and 1507  $\text{cm}^{-1}$  increase with time, since the VE monomer migrates into the penetration depth, whereas the PVP bands at 1669 and 1419  $\text{cm}^{-1}$  decrease with time.

### 3.2. Analysis of results with simple Fickian diffusion

The Fickian model is usually a good first approximation for modeling the transport behaviour in polymers [30]. Fig. 5 illustrates the diffusion system used for measuring the

diffusion between PVP and VE by FTi.r.-ATR spectroscopy. The combination of Fick's second law for unsteady state and the continuity equation for one-dimensional molecular diffusion reduces to [31]:

$$\left(\frac{\partial C}{\partial t}\right) = D \left(\frac{\partial^2 C}{\partial z^2}\right) \quad (1)$$

assuming that the diffusion coefficient,  $D$ , is constant. The PVP film is so thin that the interdiffusion direction is expected to be along the  $z$ -axis only, which is the axis perpendicular to the surface of the ATR crystal. Eq. (1) has been simplified for the case where  $D$  depends only on temperature, and is independent of other parameters such as concentration, position and thermal history. The parameter  $C(z, t)$  describes the change in the concentration profile of PVP with time,  $t$ , along the  $z$ -axis. In order to solve Eq. (1), the appropriate initial and boundary conditions have to be established. Since the two layers of PVP and VE are initially unmixed and since there is no flux across the boundaries (assuming impermeable surfaces), initial and boundary conditions based on PVP are defined as follows:

$$C = 0 \text{ at } t = 0, \quad b < z \leq a$$

$$C = C_0 \text{ at } t = 0, \quad 0 \leq z \leq b$$

$$\frac{\partial C}{\partial z}(0, t) = \frac{\partial C}{\partial z}(a, t) = 0$$

where  $z$  represents the distance from the ATR crystal,  $C_0$  is the initial concentration of PVP,  $b$  is the thickness of PVP and  $a$  is the total thickness of PVP and VE. The solutions of Eq. (1) can then be obtained either by a Laplace transform or

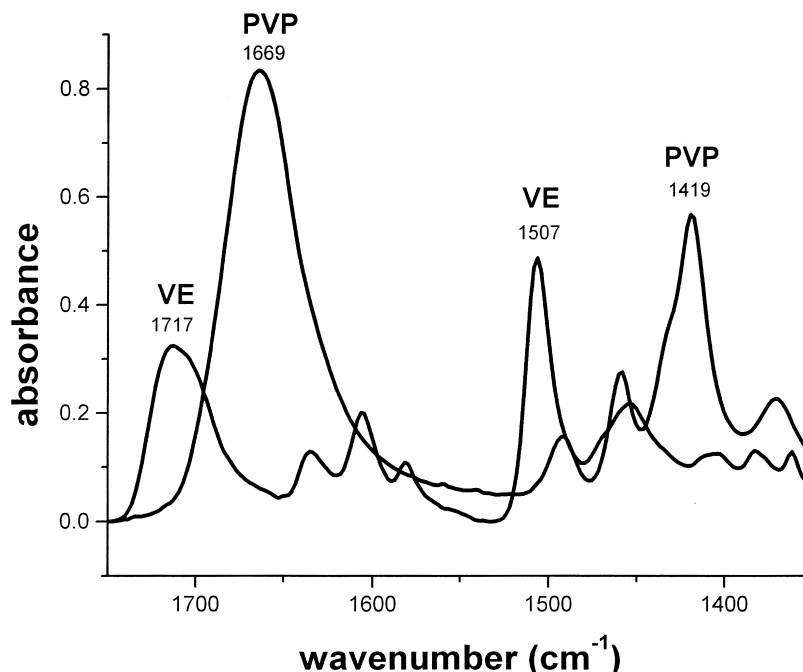


Fig. 3. FTi.r.-ATR overlapped spectra of pure PVP and VE at room temperature from 1750  $\text{cm}^{-1}$  to 13350  $\text{cm}^{-1}$ .

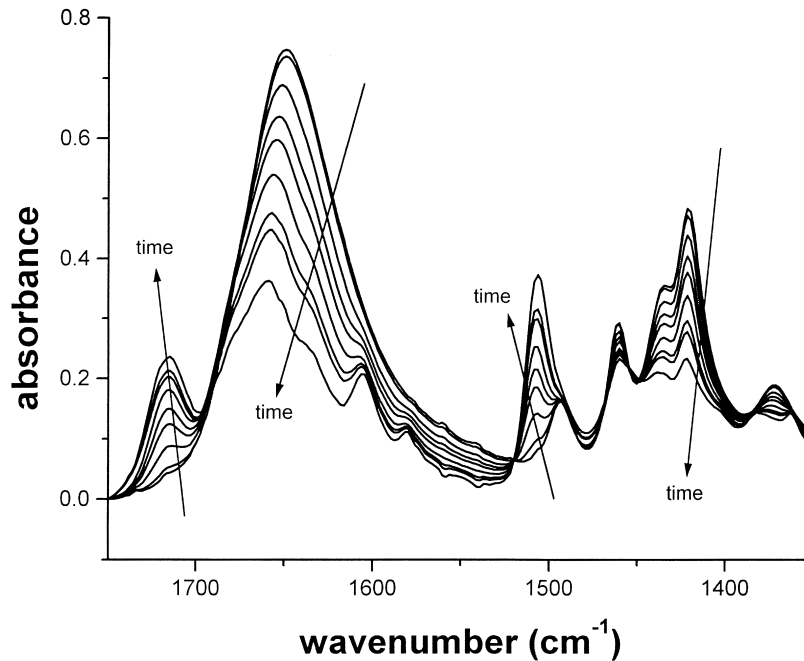


Fig. 4. Time evolution of FTIR-ATR spectra for diffusion between PVP and VE from 1750 cm<sup>-1</sup> to 1350 cm<sup>-1</sup> at 100°C. The spectra correspond to 0, 1, 2, 3, 4, 5.7, 13, 24 and 180 min of interdiffusion time.

by the method of separation of variables. It has been shown that the concentration profile of a polymer (such as PVP) within the penetration depth, given the initial and boundary conditions previously defined, can be expressed [30,31] by the following equation:

$$\frac{C(z,t)}{C_0} = \frac{b}{a} + \frac{2}{\pi} \sum_{n=1}^{\infty} \left\{ \left( \frac{1}{n} \right) \sin\left(\frac{n\pi b}{a}\right) \cos\left(\frac{n\pi z}{a}\right) \exp\left(\frac{-n^2\pi^2 Dt}{a^2}\right) \right\} \quad (2)$$

where  $n$  is the index of summation. In order to derive Eq. (2), several assumptions were made. The two phases were assumed to be completely miscible and the interface was expected to remain parallel to the boundaries. Finally, the total thickness of the system was considered to stay constant during the course of the experiment; that is no volume changes were associated with the diffusion of the monomer into the polymer. Eq. (2) does not consider any difference in size or molecular weight between the two components of the system.

The measured absorbance can be related to concentration by the following equation, valid for the ATR configuration [32]:

$$A(t) = \int_0^{\infty} \alpha \exp\left(\frac{-2z}{d_p}\right) C(z,t) S dz \quad (3)$$

where  $A(t)$  is the absorbance at any time,  $\alpha$  is the characteristic absorptivity, a constant which includes the molar extinction coefficient and the number of reflections,  $S$  is the cross-sectional area over which the measurement occurs, and  $d_p$  is the penetration depth. The exponential term in

Eq. (3) represents the exponential decay of the evanescent wave within the sample. By substituting the expression of the concentration profile of PVP (Eq. (2)) in the integral of Eq. (3), the value of the absorbance at a particular frequency at any time can be obtained. Here  $d_p$ ,  $D$ ,  $\alpha$  and  $S$  are assumed to be constant. The penetration depth is defined as:

$$d_p = \frac{\lambda}{2n_1 \pi \sqrt{(\sin\vartheta)^2 - \left(\frac{n_2}{n_1}\right)^2}} \quad (4)$$

where  $d_p$  is the penetration depth in  $\mu\text{m}$  of the infrared radiation,  $\lambda$  is the wavelength in  $\mu\text{m}$ ,  $\vartheta$  is the angle of incidence, and  $n_1$  and  $n_2$  are the refractive indices of the ATR crystal and the sample, respectively. Thus, at a

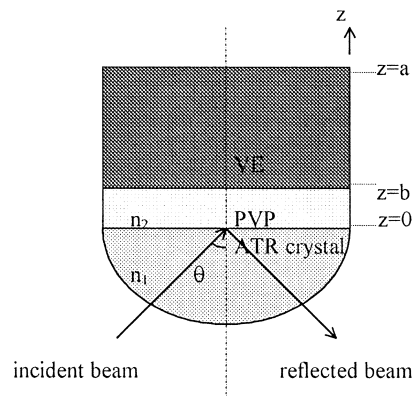


Fig. 5. Schematic of the ATR sample system for measurement of the diffusion between PVP and VE. The  $z$  is the axis perpendicular to the surface of the ATR crystal. Because the zinc selenide crystal is in the form of a hemisphere, there is a single internal reflection.

particular frequency, the penetration depth can be considered constant, as long as the refractive index remains constant throughout the experiment. However, in principle the value of the refractive index of PVP,  $n_2$ , may change as the composition of the system changes with time. Fortunately, the refractive indices of most polymers are very similar [27], thus, the penetration depth can be considered to be independent of the sample. Initially, the interface is located at  $z = b$ , which is outside the penetration depth, as illustrated in Fig. 5. When VE migrates into PVP, the concentration will change within the penetration depth. Van Alsten and Lustig [17] presented the following model relating the absorbance data to the diffusion coefficient  $D$ :

$$\frac{A(t) - A_0}{A_\infty - A_0} = 1 - \left\{ \frac{\frac{2}{\pi} \sum_{n=1}^{\infty} \left( \frac{1}{n} \right) \sin\left(\frac{n\pi b}{a}\right) \exp\left(\frac{-n^2\pi^2 Dt}{a^2}\right) \left( \frac{1 + (-1)^{n+1} \exp\left(\frac{-2a}{d_p}\right)}{1 + \left(\frac{n\pi d_p}{2a}\right)^2} \right)}{1 - \exp\left(\frac{-2b}{d_p}\right) - \frac{b}{a} \left[ 1 - \exp\left(\frac{-2a}{d_p}\right) \right]} \right\} \quad (5)$$

where  $A(t)$  is the absorbance at any time  $t$ ,  $A_0$  is the initial absorbance, and  $A_\infty$  is the equilibrium absorbance at infinite time. Eq. (5) was initially used by Van Alsten [17] and Lustig to measure the uptake of a polymer into another polymer, not realizing that this equation was specific to the polymer in contact with the ATR crystal. Nevertheless, assuming that the change in the PVP concentration at distance  $z$  and time  $t$ ,  $C(z, t)$ , is due to the diffusion of the vinyl ester monomer, the concentration of the monomer,  $C_m(z, t)$ , can be evaluated with the relation:

$$\frac{C_m(z, t)}{C_{m0}} = 1 - \frac{C(z, t)}{C_0} \quad (6)$$

where  $C_m(z, t)$  is the concentration profile of VE,  $C_{m0}$  is the initial concentration of VE at  $b < z \leq a$  and  $C_0$  is the initial concentration of PVP at  $0 \leq z \leq b$ . Eq. (6) does not take into consideration the density changes and volume changes upon mixing. Using Eq. (6), it can be shown that the same diffusion behaviour modeled by Eq. (5) applies to VE. The diffusion coefficient, which is the only unknown parameter in Eq. (5), can be determined by monitoring the intensity of characteristic absorbance bands as a function of time at a given frequency, and by fitting the absorbance–time data to the simple Fickian diffusion model Eq. (5).

Intensities of the characteristic absorption bands were obtained using a curve fitting program. The curve fitting method is a least-squares optimization routine, designed to find the best collection of individual peaks whose sum closely matches the original spectrum of overlapped bands. This curve-fitting program has to be used very cautiously, since more than one seemingly correct result

can be obtained. To verify the consistency of the results obtained by the program, the fit of a particular spectrum was carried out three times using different initial starting parameters. All data were fitted with a master curve and only those values falling directly on or close to the master curve were kept for further analysis. A shift of the carbonyl band of PVP was observed as the diffusion was going on. In this case, the peak intensity of the band, along with the shift, was followed. The diffusion coefficient of each component was then obtained by fitting the absorbance–time data to the Fickian diffusion Eq. (5) by using a simplex optimization algorithm. Reasonable agreement between the experimental data and the curve-fit results was observed at 80°C, as

illustrated in Fig. 6. The temperature dependence of the diffusion coefficient of the two components was evaluated by carrying out diffusion experiments at several temperatures, namely 80°, 90° and 100°C, and by repeating the analysis for the four characteristic peaks. The peak characteristic of the polymerization reaction, located at 940  $\text{cm}^{-1}$ , did not change at the temperatures at which the experiments were performed. The upper temperature of 100°C was chosen as a limit. Indeed, the diffusion occurs too rapidly at temperatures higher than 100°C and cannot be accurately measured with the necessary temporal resolution. One way to study the diffusion at temperatures higher than 100°C would be to increase the thickness of PVP. However, a thicker film of PVP may not have a good contact with the ATR crystal. Furthermore, at temperatures above 120°C, VE crosslinks, complicating the diffusion process and making it difficult to remove the sample from the IRE crystal without damage to the IRE crystal. The results obtained in this study are summarized in Table 1. As expected the temperature tends to increase the diffusion rates. Two diffusion coefficients were obtained for each of the PVP and VE components and were labeled  $D_{(\text{PVP})}$  and  $D_{(\text{VE})}$ , respectively. Ideally, the value of the diffusion coefficient should be the same for a given component at a fixed temperature, whatever the characteristic band. Ratios of the two characteristic bands of a given component are presented in Table 2. The results obtained for  $D_{(\text{PVP})}$  seem more consistent than those obtained for  $D_{(\text{VE})}$ , as the ratio of the two values of  $D_{(\text{PVP})}$  obtained at a given temperature is closer to unity. The difference between the two values of  $D_{(\text{VE})}$  can be due to experimental errors, such as those

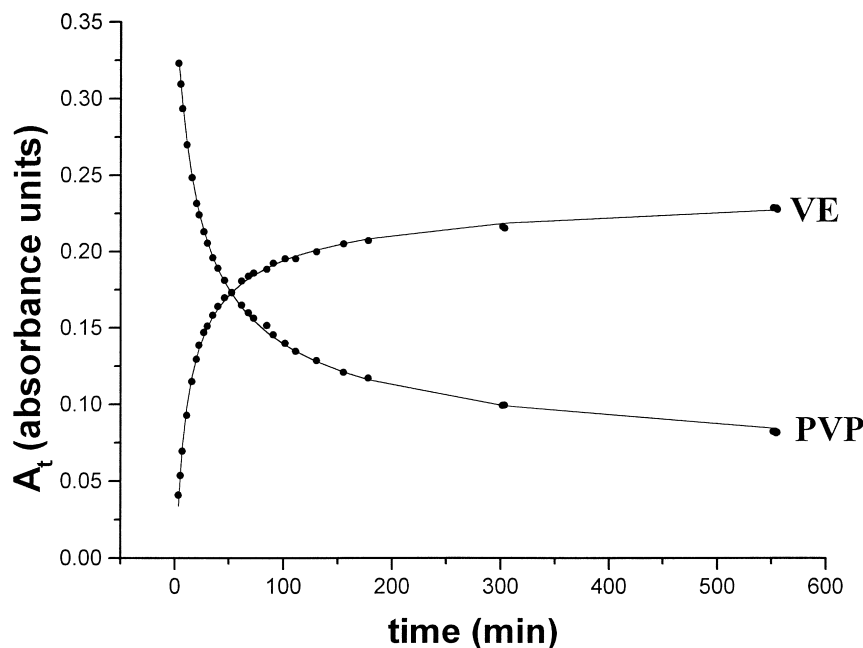


Fig. 6. Comparison of the experimental intensities of PVP and VE as a function of the interdiffusion time with those predicted by the Fickian model in equation (5) at 80°C. The dots (●) reflect the experimental data, while the solid lines represent the curve-fit. In the case of the vinyl ester, the carbonyl stretch of the vinyl ester peak at  $1717\text{ cm}^{-1}$  was used in the analysis, where  $A_0$  was taken as zero, and the penetration depth was  $1.21\text{ }\mu\text{m}$ . The best fit was obtained for a diffusion coefficient of  $5.3 \times 10^{-9}\text{ cm}^2/\text{s}$ , where  $A_\infty$  was equal to 0.251. In the case of PVP, the cyclic  $\text{CH}_2$  groups of the PVP peak at  $1419\text{ cm}^{-1}$  were used in the analysis, where  $A_0$  was taken as 0.34, and the penetration depth was  $1.46\text{ }\mu\text{m}$ . The best fit was obtained for a diffusion coefficient of  $2.6 \times 10^{-9}\text{ cm}^2/\text{s}$ , where  $A_\infty$  was equal to 0.043.

introduced during curve-fitting. An arithmetic mean of the two diffusion coefficients, corresponding to each component, was calculated at each temperature. The results are shown in Table 3. Table 4 summarizes the ratio of the diffusion coefficients of the two components. The diffusion results obtained at different temperatures were fitted with an Arrhenius type equation, as demonstrated in Fig. 7. A fit of the data with the Arrhenius equation gave an activation energy of 79 kJ/mol for the VE diffusion, and 108 kJ/mol for the PVP diffusion.

### 3.3. Molecular interactions

In addition to quantitative information concerning concentration variations, the FTi.r.-ATR technique also allows the characterization of molecular interactions occurring within the (PVP/VE) system. It is well known that the amide carbonyl group of PVP is a strong hydrogen bond acceptor [28,33]. Hydrogen bond formation results in a decrease in the strength of the C=O and OH stretching

vibrations and thus, the bands associated with the hydrogen bonded C=O and OH groups appear at lower wavenumbers than the bands associated with the free C=O and OH groups. Hydrogen bonding interactions between PVP and VE were clearly observed by ATR spectroscopy in the carbonyl region. During annealing of the (PVP/VE) sample at 100°C, the C=O stretching region of the PVP component underwent peak shifts and intensity changes as shown in Fig. 8, while the C=O band of the corresponding pure PVP, located at  $1669\text{ cm}^{-1}$ , did not change with time/temperature. Part of the shift of the PVP carbonyl band from  $1669$  to  $1650\text{ cm}^{-1}$  in the PVP/VE sample may be due to hydrogen bonding with water from the atmosphere or from the water possibly contained in the vinyl ester resin. This moisture slowly disappears as the sample is heated. Although we have measured the maximum intensity of the carbonyl peak as it shifted in frequency, the fact that extinction coefficients [34] are frequency dependent may be another possible source of error in our calculation of the

Table 1

Diffusion coefficients at different temperatures. The diffusion coefficients, based on two different infrared distinguishable bands for each component, were determined by fitting the absorbance–time data to a simple Fickian model. The relative and absolute errors are 3% and 20%, respectively

Compound	Peak ( $\text{cm}^{-1}$ )	80°C	90°C	100°C
		$D$ ( $\text{cm}^2/\text{s}$ )	$D$ ( $\text{cm}^2/\text{s}$ )	$D$ ( $\text{cm}^2/\text{s}$ )
VE	1717	$5.3 \times 10^{-9}$	$9.3 \times 10^{-9}$	$2.1 \times 10^{-8}$
VE	1507	$8.6 \times 10^{-9}$	$14.0 \times 10^{-9}$	$2.2 \times 10^{-8}$
PVP	1669	$2.2 \times 10^{-9}$	$4.9 \times 10^{-9}$	$1.4 \times 10^{-8}$
PVP	1419	$2.6 \times 10^{-9}$	$5.0 \times 10^{-9}$	$1.5 \times 10^{-8}$

Table 2

Ratio of the diffusion coefficient of a specific component based on two different spectral bands

	$D_{(\text{PVP}/1419\text{ cm}^{-1})}/D_{(\text{PVP}/1419\text{ cm}^{-1})}$	$D_{(\text{PVP}/1419\text{ cm}^{-1})}/D_{(\text{PVP}/1419\text{ cm}^{-1})}$
80°C	1.18	1.62
90°C	1.02	1.51
100°C	1.09	1.02

diffusion coefficients. Typically, the ratio of extinction coefficients of hydrogen bonded carbonyl groups to non-hydrogen bonded carbonyl groups is 1.2 to 1.5, depending on the system [35]. Unfortunately, in this particular case, it was not possible to accurately separate the diffusion and hydrogen bonding effects by curve-fitting of the carbonyl band.

### 3.4. Plasticization

At the end of the diffusion experiments, PVP had changed from a rigid solid to a white soft gel. In effect, VE has acted as a plasticizer of exceptionally high molecular weight [36–39]. The change in the glass transition temperature, as a function of the mass fraction of VE, was determined by DSC experiments. The glass transition temperatures of pure PVP and pure VE were determined to be 178° and 9°C, respectively. The change in the  $T_g$  at selected compositions of (PVP/VE) blends followed the Fox equation [40] over the range of investigation. A single  $T_g$  was observed for the blends, confirming the miscibility of PVP and VE in this range. Miscibility was also observed for a similar system by Martinez de Ilarduya et al. [41]. The change in the  $T_g$  over the entire range of the mass fraction of VE was calculated by the Fox equation [40] and is shown, along with the experimental data, in Fig. 9. Hence, during diffusion experiments, at 100°C for instance, the system would change from glassy to rubbery when the mass fraction of VE reached 35%.

## 4. Discussion

Although the fit to the experimental data appears reasonable, the ideal Fickian model described by Eq. (5) has limitations in modeling the PVP/VE system. The reason is that the ratio ( $D_{(\text{VE})}/D_{(\text{PVP})}$ ) is much greater than unity at a given temperature, as reported in Table 4. In principle, since  $D_{(\text{PVP})}$  and  $D_{(\text{VE})}$  represent mutual diffusion coefficients of PVP and VE, respectively, they should be identical [42–45]. The mutual diffusion coefficient, also called interdiffusion or collective diffusion coefficient, measures the change in

concentration of a species from its average concentration with time. This is the diffusion coefficient which is implicit in the Fick's law of diffusion. As shown in Table 4, at 80°C,  $D_{(\text{VE})}$  is almost three times greater than  $D_{(\text{PVP})}$  and at 100°C,  $D_{(\text{VE})}$  is still 1.5 times greater than  $D_{(\text{PVP})}$ . Although some errors can be expected in fitting the data, it is unlikely that such deviations would be observed entirely because of experimental errors. Because the polymers are miscible, there should be a change in the volume upon mixing of the two components. Since Eq. (5) was based on the assumption of constant volume/density, this may explain the discrepancy between the diffusion coefficients of the PVP and the VE and why this difference diminishes with increasing temperature, as the strength of hydrogen bonding interactions decreases with temperature. Consequently, when using FTi.r.-ATR spectroscopy to measure mutual diffusion coefficients, it may be a good idea to select at least two peaks for each component to verify the consistency of the diffusion coefficients at a given temperature. Typical diffusion studies cited in the literature show that only one peak is generally analyzed [17,46,47], and this peak is the one corresponding to the uptake component, i.e. vinyl ester monomer in our case. However, the results obtained for the polymer directly in contact with the ATR crystal seem more accurate, based on the quality and consistency of the fit. Interestingly, the results of the Fickian model, Eq. (5), are somewhat consistent with the range found in the literature for diffusion in PVP. While the average diffusion coefficient of the PVP/VE system in our study was on the order of  $2 \times 10^{-8}$  cm<sup>2</sup>/s at 100°C, the Polymer Handbook [48] reports a value of  $9.6 \times 10^{-7}$  cm<sup>2</sup>/s for the diffusion coefficient of water in PVP at 25°C. Oyama [49] estimated the diffusion coefficient for the (PVP/VE) system to be on the order of  $1.5 \times 10^{-8}$  cm<sup>2</sup>/s at 150°C after 5 min for a completely cured system, based on the results obtained by EMP. The value of the activation energy, between 62 and 99 kJ/mol found in this study, is consistent with activation energies reported in the literature for similar systems. For example, the activation energy for diffusion of various solvents in PMMA ranged from 79 to 146 kJ/mol [50], and that of *bis*(2-ethylhexyl)phthalate in PVC was

Table 3

Average diffusion coefficients at different temperatures. The diffusion coefficients obtained for each of the PVP and VE components are labeled  $D_{(\text{PVP})}$  and  $D_{(\text{VE})}$ , respectively

$D$ (cm <sup>2</sup> /s)	80°C	90°C	100°C
$D_{(\text{VE})}$	$7.0 \times 10^{-9}$	$11.7 \times 10^{-9}$	$2.2 \times 10^{-8}$
$D_{(\text{PVP})}$	$2.4 \times 10^{-9}$	$4.9 \times 10^{-9}$	$1.5 \times 10^{-8}$

Table 4

Ratio of ( $D_{(\text{VE})}/D_{(\text{PVP})}$ ). The diffusion coefficients obtained for each of the PVP and VE components are labeled  $D_{(\text{PVP})}$  and  $D_{(\text{VE})}$ , respectively

	$D_{(\text{VE})}/D_{(\text{PVP})}$
80°C	3
90°C	2.4
100°C	1.5



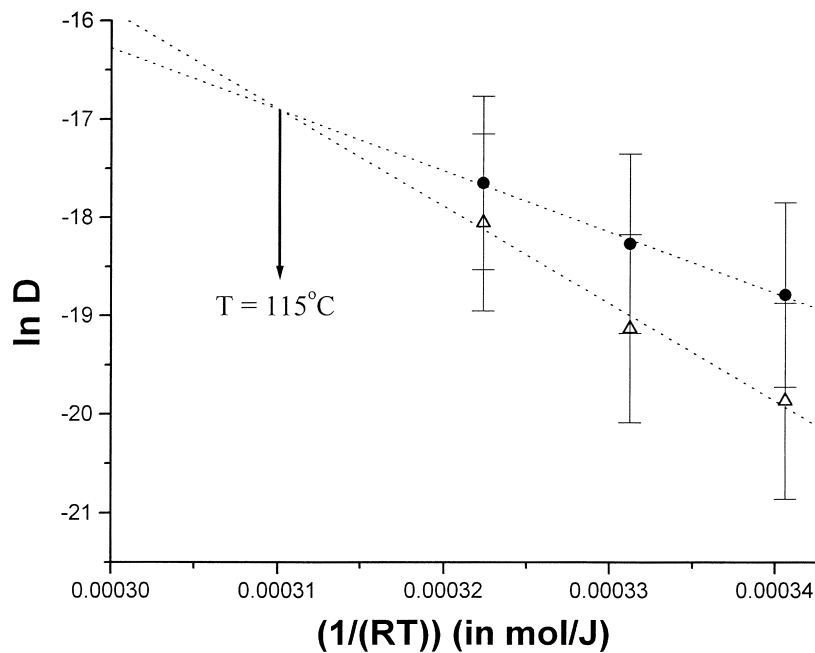


Fig. 7. Use of the Arrhenius equation for PVP ( $\Delta$ ) and VE ( $\bullet$ ) based on the results given in Table 3. The fit of PVP was obtained with a pre-exponential factor of  $1.06 \times 10^7$  cm<sup>2</sup>/s and an activation energy of 99 kJ/mol. The fit of VE was obtained with a pre-exponential factor of 11.20 cm<sup>2</sup>/s and an activation energy of 62 kJ/mol. The intercept of the two dotted lines corresponded to a temperature of 115°C.

measured as 121 kJ/mol [51]. One example of molecular transport of middle-size molecules is that of the diffusion of erucamide, molecular weight 337 g/mol, in isotactic polypropylene [52], where the activation energy was 100 kJ/mol. The activation energy of diffusion of polymers within polymers is typically lower. For example, an activation energy of 49 kJ/mol was found for the (PVC/poly(caprolactone)) system [53].

Another source of data comparison is the interfacial thickness, which is given by the following relation [54]:

$$d = 2\sqrt{2Dt} \quad (7)$$

where  $d$  is the interfacial thickness and  $D$  is the mutual diffusion coefficient. Eq. (7) was originally derived by Crank [31], considering both sides of the interface as contributing to the interphase thickness. In the present analysis,

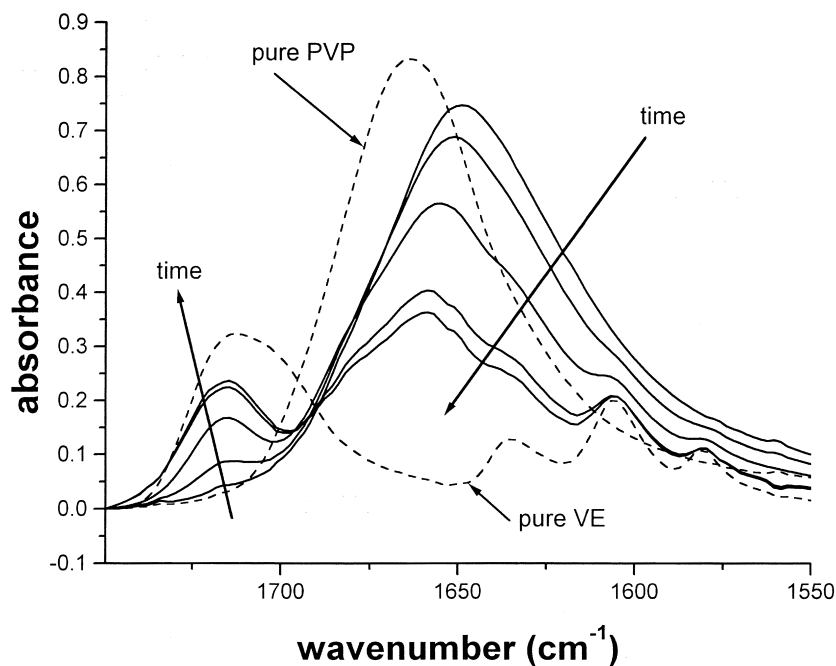


Fig. 8. Time evolution spectra in the carbonyl region during the diffusion between PVP and VE at 100°C. The spectra correspond to 0, 2, 5, 53 and 180 min of interdiffusion time. The spectra of the pure components 100°C are also given for comparison.

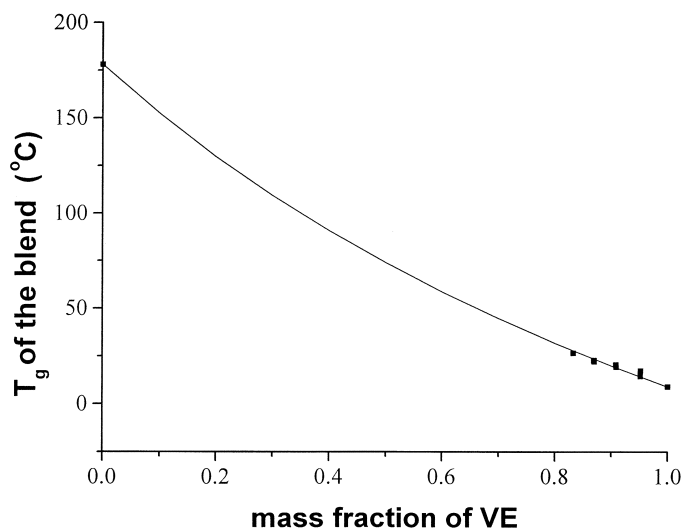


Fig. 9.  $T_g$  as a function of the mass fraction of VE. The squares (■) represent the experimentally obtained  $T_g$ , and the solid line is predicted by the Fox equation. The experimental values of the glass transition temperature were obtained by DSC experiments. The  $T_{gS}$  of pure PVP and pure VE were determined to be 178° and 9°C, respectively.

this equation would be:

$$d = \sqrt{2Dt} \quad (8)$$

Eq. (8) applies to a symmetrical profile only, i.e. for the case where the diffusion coefficients for both components are equal. From Table 4, one can see that, as the temperature increases, the difference between  $D_{(PVP)}$  and  $D_{(VE)}$  decreases. The temperature at which  $D_{(PVP)}$  and  $D_{(VE)}$  are exactly identical was calculated by the Arrhenius relation, and is shown in Fig. 7. This temperature was equal to  $115^\circ \pm 18^\circ\text{C}$ , given the 20% absolute error in determining the diffusion coefficients. The value of the resulting diffusion coefficient was equal to  $4.4 \times 10^{-8} \text{ cm}^2/\text{s}$ . At this temperature, the vinyl ester monomer is not expected to polymerize without an initiator. Indeed, DSC measurements determined that the polymerization temperature was about  $128^\circ\text{C}$  at a heating rate of  $10^\circ\text{C}/\text{min}$ . Estimates of the thickness of the polymer interphase, based on the Fickian diffusion model, yielded a value on the order of 7 mm after 5 min at  $115^\circ\text{C}$ . This is consistent with the EMP result obtained by Oyama [49], who measured an interphase thickness of 30 mm when the (PVP/VE) system was polymerized at  $150^\circ\text{C}$ .

Finally, we need to consider the fact that the  $T_g$  of PVP was constantly evolving during the experiment. The change in the  $T_g$  as a function of interdiffusion time can also be determined from the FTi.r.-ATR results. The mean concentration of PVP at a given time can be calculated from the following expression:

$$\langle C(t) \rangle_{\text{PVP}} = \frac{\int_0^\infty C_{\text{PVP}}(z, t) \exp\left(\frac{-2z}{d_{\text{pPVP}}}\right) \alpha_{\text{PVP}} S_{\text{PVP}} dz}{\int_0^\infty \exp\left(\frac{-2z}{d_{\text{pPVP}}}\right) \alpha_{\text{PVP}} S_{\text{PVP}} dz} \quad (9)$$

where  $\langle C(t) \rangle_{\text{PVP}}$  is the mean concentration of PVP,  $C_{\text{PVP}}(z, t)$  is the concentration profile of PVP,  $d_{\text{pPVP}}$  is the penetration

depth of the characteristic PVP infrared band,  $\alpha_{\text{PVP}}$  is the characteristic absorptivity of PVP, and  $S_{\text{PVP}}$  is the cross-sectional area of PVP. The numerator corresponds to the expression of the absorbance of PVP,  $A_{\text{PVP}}(t)$ , for a given time, as defined by Eq. (3). The cumulative concentration of VE,  $\langle C(t) \rangle_{\text{VE}}$ , can be defined similarly. The mole fraction of VE at a particular interdiffusion time,  $\text{mol}f_{\text{VE}}(t)$ , can then be calculated easily, assuming that  $d_{\text{pVE}}$ ,  $d_{\text{pPVP}}$ ,  $\alpha_{\text{VE}}$ , and  $\alpha_{\text{PVP}}$  remain constant. Since the cross-sectional area is the same for PVP and VE, the expression of  $\text{mol}f_{\text{VE}}(t)$  is:

$$\text{mol}f_{\text{VE}}(t) = \frac{A_{\text{VE}}(t)}{\{A_{\text{VE}}(t)\} + \left\{ \left( \frac{d_{\text{pVE}}}{d_{\text{pPVP}}} \right) \left( \frac{\alpha_{\text{VE}}}{\alpha_{\text{PVP}}} \right) A_{\text{PVP}}(t) \right\}} \quad (10)$$

Let us apply Eq. (10) to the calculation of the mole fraction of carbonyl groups. The carbonyl groups of PVP and VE have vibrational frequencies at  $1669$  and  $1717 \text{ cm}^{-1}$ , respectively. As a first approximation, one can assume that  $\alpha_{\text{PVP}}$  and  $\alpha_{\text{VE}}$  are identical, since they correspond to the same functional groups [35]. The results obtained at  $80^\circ\text{C}$  based on the carbonyl groups of VE and PVP using Eq. (10) are shown in Fig. 10. The Fox equation [40] relates the  $T_g$  to the mass fraction of VE. In order to express the  $T_g$  as a function of the interdiffusion time, a relationship between the mole fraction of VE carbonyl groups and the mass fraction of VE has to be established. Since there are 9910 carbonyl groups in one mole of PVP and two carbonyl groups in one mole of VE, the mole fraction of VE carbonyl groups,  $\text{mol}f_{\text{VE}(C=O)}(t)$ , can also be defined as:

$$\text{mol}f_{\text{VE}(C=O)} = \frac{2 \times \left( \frac{m_{\text{VE}}}{M_{\text{VE}}} \right)}{2 \times \left( \frac{m_{\text{VE}}}{M_{\text{VE}}} \right) + 9910 \times \left( \frac{m_{\text{VE}}}{M_{\text{PVP}}} \right)} \quad (11)$$

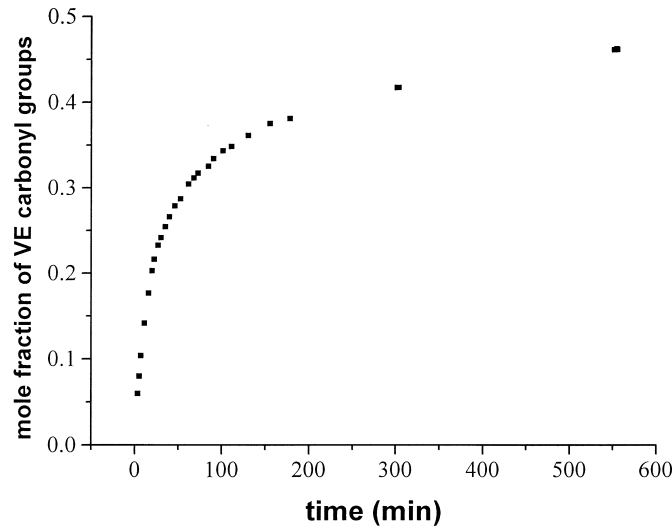


Fig. 10. Mole fraction of VE carbonyl groups as a function of interdiffusion time at 80°C calculated using Eq. (10).

where  $m_{VE}$  is the mass of VE,  $m_{PVP}$  is the mass of PVP,  $M_{VE}$  is the molecular weight of VE, and  $M_{PVP}$  is the molecular weight of PVP. The relationship between the mole fraction of VE carbonyl groups and the mass fraction of VE can then be easily established. The mass fraction of VE as a function of time can be calculated, and finally, by the use of the Fox equation, the glass transition temperature as a function of time can be obtained. The analysis was repeated for the three different temperatures of interest, as illustrated in Fig. 11. Interestingly enough, the  $T_g$  dropped by as much as 140°C during the diffusion process. As expected, the  $T_g$  decreased more rapidly at the higher temperature. Since mass transport is limited primarily by the  $T_g$ , the depression in the  $T_g$  must be accounted for in the diffusion model. For example, diffusion in amorphous glassy polymers generally follows case II diffusion, whereas diffusion in rubbery polymers is expected to obey Fick's law [32]. In previous

studies, case II diffusion was modeled by non-Fickian constitutive relations [18–20]. However, a recent model introduced by Rossi, Pincus and De Gennes [55], assumes that Fick's law can describe the transport in both the glassy and the plasticized regions, each region having its own constant diffusion coefficient. Nevertheless, the diffusion coefficient is expected to change by many orders of magnitude at the interface between glassy and plasticized regions. Although the apparent fit of the data seems at first reasonable, a closer inspection of Fig. 12 shows that at short interdiffusion times, the measured absorbance is lower than the one predicted by the Fickian Eq. (5), while at longer times, the absorbance is higher. Consequently, a two stage-diffusion process may be better in modeling the data. This was the approach taken by Quijada-Garrido et al. [52], who has employed two simultaneous Fickian processes, assuming a constant diffusion coefficient, in modeling the

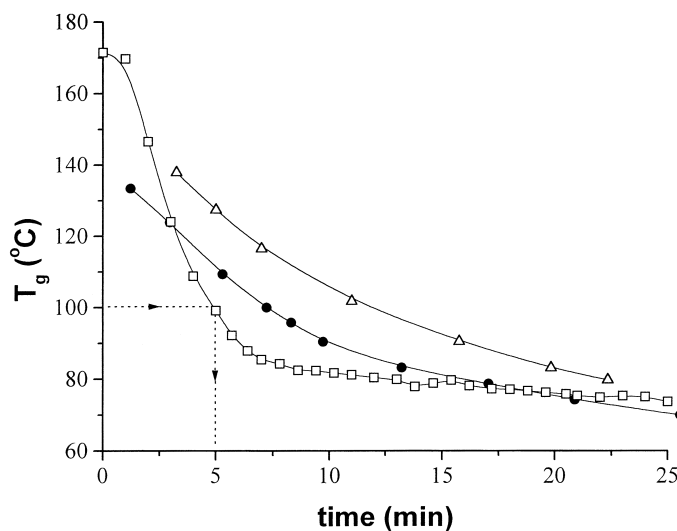


Fig. 11. System  $T_g$  as a function of interdiffusion time calculated by Eqs. (10) and (11), and by the Fox equation for different temperatures, namely 80°C ( $\Delta$ ), 90°C ( $\bullet$ ), and 100°C ( $\square$ ). The change in  $T_g$ , with interdiffusion time is shown up to 25 min. After this time, the  $T_g$  drops to 40°C.

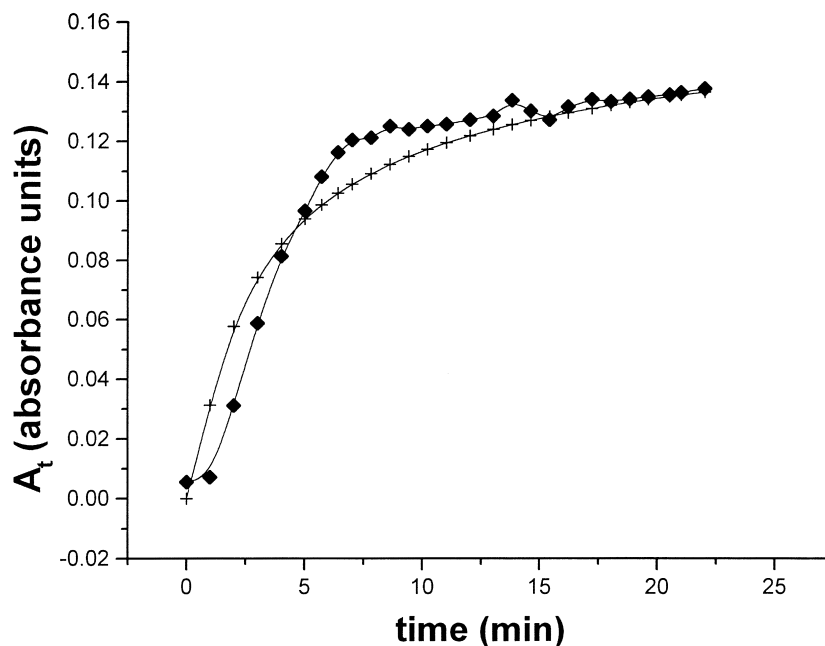


Fig. 12. Comparison of the initial experimental intensity of the carbonyl stretch of the vinyl ester peak at  $1717\text{ cm}^{-1}$  as a function of interdiffusion time with the one predicted by the Fickian model, using Eq. (5) at  $100^\circ\text{C}$ . The diamond (◆) and the cross (+) symbols are for the experimental data and the curve-fit, respectively.

diffusion of a (erucamide/isotactic polypropylene) system above  $T_g$ . Moreover, Oyama [49] observed a discontinuity in the concentration profile of PVP with VE using EMP. The concentration profile was then divided into two parts, each one being fitted by different constant diffusion coefficients, assuming Fick's law. One expects the change from a glassy to a rubbery material to have a critical effect on the value of the diffusion coefficient. From our plots in Fig. 11, the particular time at which the temperature and the  $T_g$  are identical could be determined. This time corresponds to the time at which the material changed from a glassy to a rubbery state. What is interesting is that at 5 min, the time at which the material becomes rubbery at  $100^\circ\text{C}$ , the curve-fit intercepts the experimental data points, as shown in Fig. 12. This discontinuity can be attributed to the change in the state of the material. No obvious discontinuities were noticed in the curve-fits at  $80^\circ\text{C}$  and  $90^\circ\text{C}$ , probably due to the fact that the state of the material does not change rapidly enough at lower temperatures to observe a distinct point. The diffusion Eq. (5) used in modeling the data was developed assuming a constant mutual diffusion coefficient, and thus the values of the diffusion coefficients were concentration-averaged. However, these diffusion coefficients should be strongly dependent on concentration, especially because of the change in the glass transition temperature. An exact relation between the mutual diffusion coefficient and the concentration needs to be established in order to solve the Fickian differential equation. Unfortunately, no theoretical models have been proposed to date. Samus and Rossi [37] suggested recently a Fermi function form for the expression of the diffusion coefficient in the transition region between the glassy and the rubbery state. Its

expression was given by:

$$D(\phi) = D_0 + \frac{D_1 - D_0}{1 + \exp(-L(\phi - \tilde{\phi}))} \quad (12)$$

where  $D(\phi)$  is the diffusion coefficient in the transition region,  $D_0$  is the diffusion coefficient in the glassy phase,  $D_1$  is the diffusion coefficient in the rubbery phase,  $L$  is a parameter controlling the size of the transition region,  $\phi$  is the concentration and  $\tilde{\phi}$  is the concentration above which plasticization occurs. Samus and Rossi [37] expected Fick's law to describe the transport in both the glassy and the rubbery states. If the data points recorded at and before 5 min in Fig. 12 are canceled for the vinyl ester peak at  $1717\text{ cm}^{-1}$  at  $100^\circ\text{C}$ , then the value of the diffusion coefficient is equal to  $3.7 \times 10^{-8}\text{ cm}^2/\text{s}$ , when curve-fitting the truncated data set with Eq. (5). This value corresponds to the diffusion coefficient in the rubbery state. As a reminder, the overall value of the diffusion coefficient was determined to be  $2.1 \times 10^{-8}\text{ cm}^2/\text{s}$ , about 40% lower. It was impossible to evaluate the diffusion coefficients in the glassy and the transition regions. Indeed, in order to get the value of the diffusion coefficient in the glassy state, an estimation of  $A_\infty$  is needed to solve Eq. (5). Such an estimate would be meaningless. However, one can guess that the diffusion coefficient in the glassy state will be at least one order of magnitude lower than the one in the rubbery state [55]. Furthermore, in order to get the value of the diffusion coefficient in the transition region, the dependence of the diffusion coefficient as a function of the distance has to be known to solve the Fickian differential equation. However, Eq. (12) provides only information about the dependence of

the diffusion coefficient on the concentration, not on the distance across the interphase.

## 5. Conclusion

The molecular interdiffusion across a poly(vinyl pyrrolidone)/vinyl ester monomer (PVP/VE) interface was measured experimentally by FTi.r.-ATR spectroscopy. The mutual diffusion coefficients, obtained separately for PVP and VE, differed by a temperature dependent factor, suggesting that, when there is a volume change due to mixing, the ATR method employing a simple one-dimensional Fickian model is not completely accurate. On the other hand, the absolute values of the diffusion coefficients were consistent with the range of values found in the literature for diffusion in polymers, employing other methods. Finally, even though a reasonable fit of the spectral data was obtained, conceptually, we found that using constant diffusion coefficients in modeling the PVP/VE system was not appropriate. The evolution of the glass transition temperature was followed as a function of interdiffusion time by FTi.r.-ATR spectroscopy. Because the  $T_g$  of PVP drastically changed as diffusion proceeded, one would expect that the mutual diffusion coefficient should change as well. We hope to address this topic in our future studies.

## Acknowledgements

We extend our sincere thanks to Dr. Sukhtej S. Dhingra for his help with the curve fitting software and to Kermit Kwan for running the DSC experiments. This work was supported by the National Science Foundation Science and Technology Center for High Performance Polymeric Adhesives and Composites at Virginia Tech under grant no. DMR-9120004.

## References

- [1] Lesko JJ, Rau A, Riffle JS. Proceedings of the 10th Technical Conference of the American Society for Composites, 1995:53.
- [2] Han CD, Lem K-W. J Appl Polym Sci 1984;29: 1879.
- [3] Dirand X, Hilaire B, Lafontaine E, Mortaigne B, Nardin M. Composites 1994;25:645.
- [4] Li H, Rosario AC, Davis SV, Glass T, Holland TV, Davis RM, Lesko JJ, Riffle JS, Florio J. J Adv Mat 1997;28:55.
- [5] Xie M, Weitzsacker CL, Rich M, Drzal LT. Proceedings of the 20th Annual 'Anniversary' Meeting of the Adhesion Society, 1997, 555.
- [6] Voyutskii SS. Autoadhesion and adhesion of high polymers. New York: Wiley, 1963.
- [7] Lesko JJ, Swain RE, Cartwright JM, Chin JW, Reifsnider KL, Dillard DA, Wightman JP. J Adh 1994;45:43.
- [8] Oyama HT, Davis SV, Wightman JP, Riffle JS. Polymer Preparation 1996;37(2):79.
- [9] Oyama HT, Lesko JJ, Wightman JP. J Polym Sci: Part B, Polym Phys 1997;35:331.
- [10] Oyama HT, Wightman JP. Polymer 1998, in press.
- [11] Kramer EJ, Green P, Palmström CJ. Polymer 1984;25:473.
- [12] Mills PJ, Green PF, Palmström CJ, Mayer JW, Kramer EJ. Journal of Polymer Science and Polymer Physics 1986;24:1.
- [13] Sauer BB, Walsh DJ. Macromolecules 1991;24:5948.
- [14] Jordan EA, Ball RC, Donald AM, Fetters LJ, Jones RAL, Klein J. Macromolecules 1988;21:235.
- [15] Gilmore PT, Falabella R, Laurence RL. Macromolecules 1980;13:880.
- [16] Kanetakis J, Fytas G. Macromolecules 1989;22:3452.
- [17] Van Alsten JG, Lustig SR. Macromolecules 1992;25:5069.
- [18] Jabbari E, Peppas NA. Macromolecules 1993;26:2175.
- [19] Jabbari E, Peppas NA. J Mat Sci 1994;29:3969.
- [20] Jabbari E, Peppas NA. J Adh 1993;43:101.
- [21] Jabbari E, Peppas NA. Polym Int 1995;38:65.
- [22] Fieldson GT, Barbari TA. Polymer 1993;34:1146.
- [23] Fieldson GT, Barbari TA. AIChE Journal 1995;41:795.
- [24] Cogan Farinas K, Doh L, Venkatraman S, Potts RO. Macromolecules 1994;27:5220.
- [25] Semwal RP, Banerjee S, Chauhan LR, Bhattacharya A, Rao NBSN. J Appl Polym Sci 1996;60:29.
- [26] Huang SU, Barbari TA, Sloan JM. J Polym Sci Part B, Polym Phys 1997;35:1261.
- [27] Seferis JC. In: Polymer Handbook, 3rd ed. New York: Wiley-Interscience, 1989:VI/461.
- [28] Janarthanan V, Thyagarajan G. Polymer 1992;33:3593.
- [29] Alpert NL, Keiser WE, Szymanski HA. IR—Theory and Practice of Infrared Spectroscopy. New York: Plenum/Rosetta, 1973.
- [30] Rideal EK. Diffusion in and through solids. The Cambridge Series of Physical Chemistry, 1951.
- [31] Crank J. The mathematics of diffusion, 2nd edn. Oxford: Clarendon Press, 1975.
- [32] Van Alsten JG. Trends in Polym Sci 1995;3:272.
- [33] Robinson BV, Sullivan FM, Borzelleca JF, Schwartz SL. PVP—a critical review of the kinetics and toxicology of polyvinylpyrrolidone (Povidone). Lewis Publishers, 1990.
- [34] Willis HA, Van der Maas JH, Miller RGJ, editors. Laboratory methods in vibrational spectroscopy, 3rd ed. New York: Wiley, 1987:18.
- [35] Coleman MM, Graf JF, Painter PC. Specific interactions and the miscibility of polymer blends. Lancaster: Technomic Publishing, 1991.
- [36] Rossi G. Trends in Polym Sci 1996;4:337.
- [37] Samus MA, Rossi G. Macromolecules 1996;29:2275.
- [38] Sears JK, Touchette NW. In: Mark HF, Bikales NM, Overberger CG, Menges G, editors. Encyclopedia of polymer science and engineering, 2nd ed. suppl. vol. New York: Wiley, 1989:568.
- [39] Sears JK, Touchette NW, Darby JR. In: Applied polymer science. ACS Symposium Series. Washington, DC: American Chemical Society, 1985:611.
- [40] Sperling LH. Introduction to physical polymer science, 2nd ed. New York: Wiley, 1992.
- [41] Martinez de Ilarduya A, Iruin JJ, Fernandez-Berridi MJ. Macromolecules 1995;28:3707.
- [42] Brochard-Wyart F. Fundamentals of adhesion. New York: Plenum Press, 1991:181.
- [43] Binder, K. and Sillescu, H., in Encyclopedia of Polymer Science and Engineering, 2nd Edn, ed. H. F. Mark, N. M. Bikales, C. G. Overberger and G. Menges, Suppl. Vol. Wiley, New York, 1989, p. 297.
- [44] Chih-ch'iiian P. Journal of Applied Chemistry of the USSR 1989;62:2320.
- [45] Koros WJ, Hellums MW. In: Mark HF, Bikales NM, Overberger CG, Menges G, editors. Encyclopedia of polymer science and engineering, 2nd ed., suppl. vol. New York: Wiley, 1989:724.
- [46] Lustig SR, Van Alsten JG, Hsiao B. Macromolecules 1993;26:3885.
- [47] Van Alsten JG, Lustig SR, Hsiao B. Macromolecules 1995;28:3672.

- [48] Lechner MD, Steinmeier DG. In: Brandrup J, Immergut EH, editors. *Polymer handbook*, 3rd ed. New York: Wiley-Interscience, 1989:VII/77.
- [49] Oyama HT, to be published.
- [50] Arnould D, Laurence RL. *Industrial Engineering Chemistry Research* 1992;31:218.
- [51] Storey RF, Mauritz KA, Cole BB. *Macromolecules* 1991;24:450.
- [52] Quijada-Garrido I, Barrales-Rienda JM, Frutos G. *Macromolecules* 1996;29:7164.
- [53] Gilmore PT, Falabella R, Laurence RL. *Macromolecules* 1980;13:880.
- [54] Wu S, Chuang H-K, Dae Han C. *J Polym Sci: Polymer Physics Edition* 1986;24:143.
- [55] Rossi G, Pincus PA, De Gennes P-G. *Europhysics Letters* 1995;32:391.